Negative Differential Resistance in a Hybrid Silicon-Molecular System: Resonance between the Intrinsic Surface-States and the Molecular Orbital

Weihua Wang, Yongfei Ji, Hui Zhang, Aidi Zhao, Bing Wang,* Jinlong Yang, and J. G. Hou*

Hefei National Laboratory for Physical Sciences at the Microscale, University of Science and Technology of China, Hefei, Anhui 230026, China

ABSTRACT

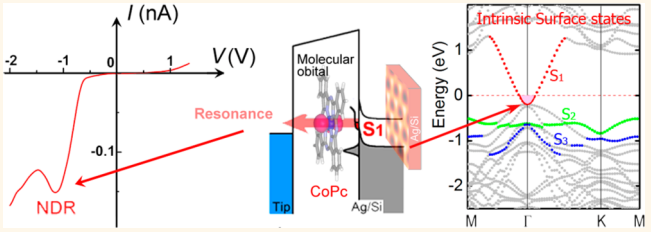

It has been a long-term desire to fabricate hybrid silicon-molecular devices by taking advantages of organic molecules and the existing silicon-based technology. However, one of the challenging tasks is to design applicable functions on the basis of the intrinsic properties of the molecules, as well as the silicon substrates. Here we demonstrate a silicon-molecular system that produces negative differential resistance (NDR) by making use of the well-defined intrinsic surface-states of the Si (111)-$\sqrt{3} \times \sqrt{3}$-Ag (R3-Ag/Si) surface and the molecular orbital of cobalt(II)−phthalocyanine (CoPc) molecules. From our experimental results obtained using scanning tunneling microscopy/spectroscopy, we find that NDR robustly appears at the Co^{2+} ion centers of the CoPc molecules, independent of the adsorption configuration of the CoPc molecules and irrespective of doping type and doping concentration of the silicon substrates. Joint with first principle calculations, we conclude that NDR is originated from the resonance between the intrinsic surface-state band S_1 of the R3-Ag/Si surface and the localized unoccupied Co^{2+} d_{z^2} orbital of the adsorbed CoPc molecules. We expect that such a mechanism can be generally used in other silicon-molecular systems.

KEYWORDS: hybrid silicon-molecular electronics · negative differential resistance · surface-states · Si(111)-$\sqrt{3} \times \sqrt{3}$-Ag · cobalt(II)−phthalocyanine · scanning tunneling microscopy/spectroscopy · density functional theory calculation

Because of the ongoing miniaturization of semiconductor devices, molecular electronics is foreseen as a possible way to assemble functional molecules on silicon to form hybrid silicon-molecular electronics.[1−10] In this perspective, functional organic molecules on silicon surfaces are promising candidates as they can be implemented in the existing technology for fabrication of silicon-based micro- and nanostructured devices.[11−15] Although a lot of works have been done on the assembly of molecular structures on silicon or silicon-based surfaces,[16−22] the electronic properties of such silicon-molecular systems are mainly studied separately by considering either the Si substrate or the adsorbed molecules. Only a few of previous works have been done on the electron transport between molecules and Si electrodes by considering both of their electronic properties. For example, styrene, cyclopentene, and 2,2,6,6-tetramethyl-1-piperidinyloxy molecules on Si lead to a negative differential resistance (NDR),[23−25] where the occurrence of NDR was explained by using a model of resonance between the molecular level and the energy bands of Si when the molecular level moves in and out of alignment with the band edges under the applied electric fields.[26] However, it was still argued that for instance, the frontier energy levels of cyclopentene on the *p*-type Si(001) are calculated to be independent of the applied electric fields due to the strong coupling of the molecule to the Si substrate.[27]

Because of the existence of the dangling bonds on bare silicon surfaces, the electronic properties of adsorbed molecules can be strongly modified by the interactions between molecules and silicon surfaces,[28,29] and the molecules can even be dissociated.[30,31] Alternatively, passivated silicon surfaces, such as the Si(100):H surface,[32] Si(111)-$\sqrt{3} \times \sqrt{3}$-B surface,[33] and Si(111)-$\sqrt{3} \times \sqrt{3}$-Ag surface (abbreviated as R3-Ag/Si),[34−40] were introduced as inert supporting surfaces for molecular structures, while the effect of the intrinsic electronic properties of the surfaces was seldom taken into consideration in such

* Address correspondence to bwang@ustc.edu.cn, jghou@ustc.edu.cn.

Received for review May 13, 2012 and accepted July 13, 2012.

Published online July 13, 2012
10.1021/nn302107k

systems.[41] The R3-Ag/Si surface is one of the most studied passivated surfaces. Actually, the R3-Ag/Si surface possesses well-characterized surface-state (SS) bands, S_1, S_2, and S_3, near the Fermi level (E_F).[42,43] The SS band S_1, with its bottom located at around 0.3 eV below the E_F, is highly upward dispersive and partially filled by electrons, irrespective of doping type and doping concentration in the bulk, so that the bulk bands bend upward in the space-charge layer (SCL), and the E_F of the surface is pinned by the SS band S_1.[44−50] The SS bands S_2/S_3 (degenerated at the Γ point) locate at around 1.1 eV below the E_F, and an energy gap of 0.7 eV opens up between S_1 and S_2/S_3 bands.[42−50] We have observed NDR on the bare R3-Ag/Si surface due to the interplay of the localized S_2/S_3 states and the SCL; however, the appearance of NDR is highly dependent on several factors, for example, the specific sites of the surface, the doping concentration of Si substrate, and the measuring temperature.[51] It remains an open question if one can make use of such surface states to design reliable silicon-molecular devices.

Here we demonstrate that by depositing cobalt(II)−phthalocyanine (CoPc) molecules on the R3-Ag/Si surface, the NDR effect is produced robustly at the central Co^{2+} ion, which is attributed to the resonance between the SS band S_1 of the R3-Ag/Si surface and the localized Co^{2+} d_{z^2} orbital of the adsorbed CoPc molecules. Moreover, it is found that the polarity of the NDR shows no dependence on the doping type of Si substrates. Conceptually, one can generally make use of the intrinsic surface states of a passivated silicon surface to design hybrid silicon-molecular devices by choosing functional molecules with proper electronic structures.

RESULTS AND DISCUSSION

Observation of NDR at Co^{2+} Ion Centers of Adsorbed CoPc Molecules on R3-Ag/Si. Figure 1a shows a representative STM image of CoPc molecules adsorbed on a R3-Ag/Si surface. The CoPc molecules adsorb flat-lying on the surface, exhibiting the four-leaf pattern with the protruded Co^{2+} center. The orientations of the molecules can be dominantly divided into three groups. In these adsorption configurations, one of the symmetry axes of each molecule tilts clockwise by 15°, 45°, or 75° with respect to the [11$\bar{2}$] direction of the R3-Ag/Si surface (see Supporting Information). Considering the 3-fold symmetry of the R3-Ag/Si surface and 4-fold symmetry of the CoPc molecule, we find that these different orientations are symmetrically equivalent, that is, the CoPc molecules have almost a determined orientation with one symmetry axis tilting by 15° from the ⟨11$\bar{2}$⟩ directions, whereas the adsorption sites of the CoPc molecules show variations from one molecule to another. Figure 1b shows a magnified STM image of four

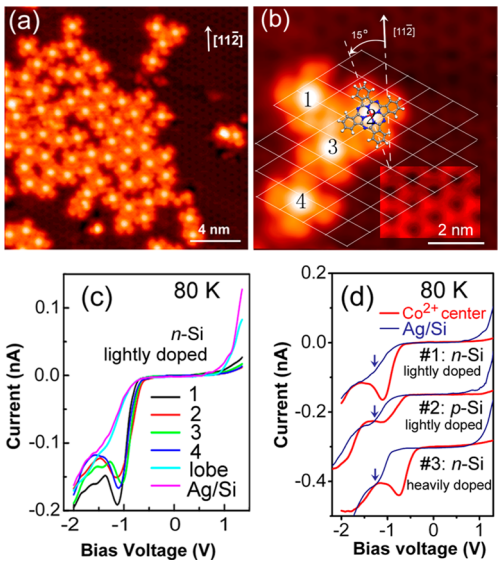

Figure 1. (a) STM image of CoPc molecules adsorbed on an R3-Ag/Si surface with lightly doped *n*-type wafer. (b) Magnified STM image showing four CoPc molecules with different adsorption configurations. The lattice of the R3-Ag/Si surface and CoPc structural model are superimposed in the image. (c) Representative *I*−*V* curves measured at the Co^{2+} ion centers and the benzene lobe of CoPc molecules shown in panel b, in comparison with the *I*−*V* curve taken at the R3-Ag/Si surface. Acquired at −2.2 V, 0.2 nA, at 80 K. (d) Representative *I*−*V* curves measured at the Co^{2+} ion centers of CoPc molecules on R3-Ag/Si surfaces of different samples at 80 K: (1) lightly doped *n*-type Si wafer (−2.2 V and 0.2 nA), (2) lightly doped *p*-type Si wafer (−2.15 V and 0.1 nA), and (3) heavily doped *n*-type Si wafer (−2.0 V and 0.2 nA). The blue arrows mark the shoulder feature of the *I*−*V* curves correspondingly taken from the R3-Ag/Si substrates. The curves taken from different samples are shifted from each other for clarity.

CoPc molecules in different adsorption configurations, superimposed with the lattice of the R3-Ag/Si surface[43,48,52−54] and the CoPc structural model. The four molecules shown in Figure 1b lie with their Co^{2+} ion centers on top of the Ag atom or on the center of the Ag triangle, and with orientation of ±15° with respect to the [11$\bar{2}$] direction of the R3-Ag/Si surface.

We measured the current−voltage (*I*−*V*) curves by locating the STM tip at the Co^{2+} ion centers and the benzene lobes of CoPc molecules on a lightly doped *n*-type wafer (sample no. 1). Figure 1c shows representative *I*−*V* curves measured at the Co^{2+} ion centers of the four CoPc molecules in Figure 1b, measured at 80 K. It is observed that the Co^{2+} ion centers exhibit the NDR, with the current peaks at around −1.1 V. The peak position of the NDR (NDR positions) and the peak-to-valley ratio just slightly vary with the different locations of the Co^{2+} ion centers with respect to the R3-Ag/Si lattice. In contrast, the *I*−*V* curve measured at the benzene lobe of CoPc molecule only shows a shoulder feature at around −1.3 V, giving nearly the same feature as the one at the R3-Ag/Si surface. The shoulder feature in the *I*−*V* curves taken at the R3-Ag/Si surface (and similarly at the benzene lobe) is attributed to the

contribution of the SS bands S_2/S_3 of the R3-Ag/Si surface, as we reported before.[51]

We also conducted the measurements by using a lightly doped *p*-type Si wafer (sample no. 2) and a heavily doped *n*-type Si wafer (sample no. 3) at 80 K. The representative results are summarized in Figure 1d. It is observed that the NDR only occurs at the negative bias at the Co^{2+} ion center in the samples either with the *p*-type or with the *n*-type Si substrates, indicating that the doping type of the silicon substrate does not affect the bias polarity of the NDR at the Co^{2+} ion center. The NDR position obtained at the Co^{2+} ion center in sample no. 2 (with the lightly doped *p*-type wafer) occurs at around −1.1 V, similar to that in sample no. 1 (with the lightly doped *n*-type wafer) (Figure 1d). However, the NDR occurs at around −0.75 V in sample no. 3 (with the heavily doped *n*-type Si wafer). The NDR positions are all at smaller bias voltages than the positions of the SS bands S_2/S_3 (marked by the arrows) in these samples. It indicates that the NDR observed at Co^{2+} ion center should not be caused by the localized SS bands S_2/S_3, since the E_F of the STM tip has not swept to the energy levels of the SS bands S_2/S_3 when the NDR occurs. We also performed the experiment by using metal-free phthalocyanine (H_2Pc) instead of CoPc; however, NDR was not observed in H_2Pc molecules, neither at the molecular center nor at the benzene ring (see Supporting Information). This means that the specific electronic states of the CoPc molecules should be crucial for the NDR effect.

In the measurement of *I*−*V* curves, the NDR may also be caused by the overlap of a sharp feature in the local density of states of an STM tip,[55] or an STM tip with a captured molecule at the apex.[56] In such situations, the *I*−*V* curves should be strongly dependent on the tip conditions. In our measurements, we changed several different tips. Before and after the measurements at the molecules, we always checked the *I*−*V* curves acquired at the R3-Ag/Si surface, which was used as a reference.[51] The NDR observed at Co^{2+} ion center of CoPc does not show any dependence on the tips as long as the tips correctly produce the *I*−*V* curves reflecting the feature of the R3-Ag/Si surface. Therefore, we believe that the NDR should not be due to some special situations of the tips. On the basis of our observations, it strongly suggests that the molecule−substrate interface should play a dominant role,[42,57] where the alignment of the molecular energy levels with the surface-states of R3-Ag/Si can be the key to the understanding of our observations.

Mechanism of the NDR at Co^{2+} Ion Centers of CoPc on R3-Ag/Si Surface. *Density Functional Theory (DFT) Calculations for CoPc and H_2Pc on Ag/Si Surface.* To understand our observations, we performed DFT calculations for the CoPc and H_2Pc molecules on the R3-Ag/Si surface. The optimized structure shown in Figure 2a adopts an

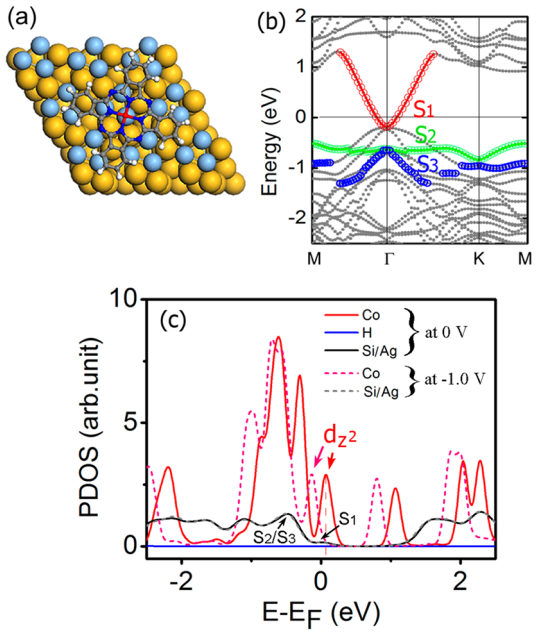

Figure 2. (a) Structural model of CoPc (or H_2Pc) molecule on the R3-Ag/Si surface. The Si, Ag, C, N, H, and Co atoms are drawn in yellow, light blue, gray, blue, white, and red colors, respectively. (b) Calculated band structure of R3-Ag/Si surface. The SS bands S_1, S_2, and S_3 are marked by colored symbols. The bottom of the S_1 band is set to be 0.3 eV below E_F. (c) Calculated PDOS of central Co and H of the adsorbed CoPc and H_2Pc molecule, and PDOS of the R3-Ag/Si surface at equilibrium (solid lines) and electric field of −0.2 V/Å (dashed lines), respectively. The lines are almost overlapped for the Ag/Si under zero bias (black) and under −0.2 V/Å electric field or −1.0 eV bias (dashed gray).

adsorption configuration by locating the molecular center on the top of a Ag atom, with the molecular orientation tilting from the $[11\bar{2}]$ direction by 15° according to our experimental results. Figure 2b shows the calculated band structure of R3-Ag/Si, which accords well with the previously reported band structure of R3-Ag/Si with different calculation methods.[43,54] The surface-state bands are also marked in Figure 2b. The partial density of states (PDOS) of the R3-Ag/Si surface and the central Co^{2+} ion (or central H) of the adsorbed CoPc (or H_2Pc) at equilibrium and electric field of −0.2 V/Å are given in Figure 2c. Here, we assume a tip−sample distance of 5 Å, corresponding to an applied sample bias voltage of −1.0 V for the electric field of −0.2 V/Å. Some other adsorption configurations by locating the Co^{2+} center at different sites basically give similar results (see Supporting Information), indicating that the variation of adsorption sites just slightly affects the electronic structures of the molecules.

It is obtained that the lowest unoccupied molecular orbital (LUMO) is contributed by the d_{z^2} orbital of the central Co^{2+} ion, varying in the small energy range of 0.08−0.12 eV above the Fermi level with the different adsorption sites of the CoPc molecules at equilibrium. The small variation range of the d_{z^2} orbital should be

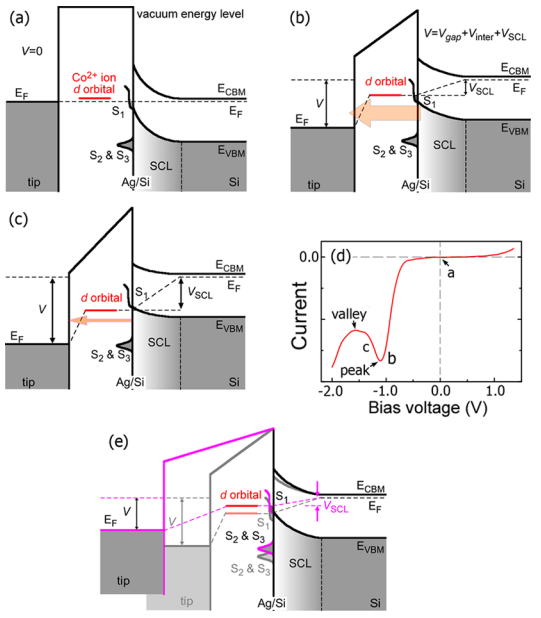

Figure 3. Schematic drawing of energy diagram (a) at equilibrium, (b) at a negative bias voltage leading to resonance between the Co^{2+} ion d orbital and SS band S_1, and (c) at higher negative bias voltage leading the Co^{2+} ion d orbital to move into the energy gap between the S_1 and the S_2/S_3. (d) The corresponding portions of the NDR and the bias voltages corresponding to the energy diagrams in panels a–c. (e) The energy diagram with a broadened tip-molecule gap, in which the Co^{2+} ion d orbital aligns the SS band S_1 at a smaller negative bias voltage. In panel e, the situation of panel b is faintly given for comparison. E_{CBM}, conduction-band minimum; E_{VBM}, valence-band maximum of Si substrate.

responsible for the slight variation of the NDR behaviors observed in Figure 1c. For simplicity, we adopt a value of 0.1 eV for the d_{z^2} orbital at equilibrium in the following discussion. In comparison, the central H atoms in H_2Pc molecule do not give any apparent state in the concerned energy range. Under the applied electric field, for example at −0.2 V/Å, the PDOS of the central Co^{2+} ion shifts downward, causing the d_{z^2} orbital below the Fermi level and to align the S_1 band. This means that a certain voltage drop may happen between the molecule and the substrate. It can be seen in the following discussion that such alignment may be the main reason of the NDR.

Energetic Interpretation of NDR Due to the Resonance between the Orbital of CoPc and the SS Band S_1. According to the calculated electronic structure of the CoPc and the surface-states of the R3-Ag/Si surface, we propose a model to interpret the NDR observed in CoPc, as shown in Figure 3. At equilibrium (zero bias applied), the localized d_{z^2} orbital of the Co^{2+} ion locates above the E_F by 0.1 eV (Figure 3a). Under an applied bias voltage (V), the voltage may drop at the tip–molecule gap (V_{gap}), at the molecule–substrate interface (V_{inter}), and at the SCL (V_{SCL}), as shown in Figure 3b. This is confirmed by the calculation of the PDOS under the electric field of 0.2 V/Å in Figure 2c. By sweeping the voltage to a certain negative bias value, once the voltage drop V_{inter} reaches 0.1 V, the d_{z^2} orbital subsequently aligns with the SS band S_1, as shown by the dashed lines in Figure 2c, leading to the resonance between them and thus resulting in a current maximum in I–V curve. With the further increasing of the bias voltage, the d_{z^2} orbital moves into the energy gap between the S_1 and the S_2/S_3 (Figure 3c), then the resonance between the molecular orbital and the S_1 is interrupted, causing the tunneling current to begin to decrease. In the gap between the S_1 and the S_2/S_3, the tunneling electrons can be mainly from the valence band of the R3-Ag/Si rather than from the S_1 state. The corresponding portions of the NDR are schematically shown in Figure 3d. Since the SS bands S_2/S_3 are still below the E_F of the tip, these states are not involved in and do not contribute to the NDR. It should be mentioned that the calculations underestimate the gap between the S_1 and the S_2/S_3 surface states (Figure 2b,c), giving that the calculated S_2/S_3 states are about 0.5 eV (at Γ) higher than the experimental results from the ARPES[44,50] and STM.[51] On the basis of the experimental fact, the discrepancy on the energy position of the S_2/S_3 should not alter our conclusion.

Here our suggestion that the voltage may drop at the molecule–substrate interface is based on the nature of the Ag passivated Si surface, where the molecules are weakly physisorbed on the surface.[34–40] At room temperature, CoPc may rapidly diffuse at a low coverage of 0.1 ML on R3-Ag/Si, and CoPc may form ordered structure at a high coverage of about 1 ML.[39] From our DFT calculations, the adsorption energy is 0.39 eV for the Co^{2+} center at the top site, 0.29 eV at the bridge site, 0.23 eV at the center of the small Ag trangle, 0.20 eV at the center of the large Ag triangle, and 0.27 eV at the hollow site (see Figure S4 in Supporting Information). The values of the adsorption energies may well support that the adsorption of CoPc on the R3-Ag/Si surface is relatively weak. It is also consistent with the shift of the PDOS of Co^{2+} ion center under an applied electric field (Figure 2c). This situation is quite different from those for molecules on the nonpassivated Si surfaces, where the adsorbed molecules may covalently couple to the Si surfaces.[23–27] As for H_2Pc, since it does not have similar energy levels near the E_F, the NDR mechanism proposed for CoPc on R3-Ag/Si is not available for H_2Pc.

The accuracy of the calculated electronic structure of CoPc can be an important issue regarding the mechanism proposed here. These years, there are a lot of experimental[58–62] and theoretical[63–66] studies on the electronic structures of metal phthalocyanines (MPc). Although the detailed information may vary in some extent from one system to another, the experimental and theoretic results for the occupied states are basically in good agreement. However, the calculations do not well describe the gap between the highest

occupied molecular orbital (HOMO) and the lowest unoccupied molecular orbital (LUMO) in comparison with the inverse photoemission results,[59,64] especially for the thin films (monolayer or submonolayer) of MPc on metal substrates. It can be attributed to the generalized gradient approximation (GGA) of Perdew, Burke, and Ernzerhof (PBE)[67] that the HOMO and LUMO do not correspond to the ionization potential or the electron affinity, respectively.[68] The energy order of the occupied orbitals from the Kohn−Sham states is in most cases in agreement among the various methods; however, the order of empty orbitals of a minimal basis set is sometimes interchanged.[69] In the case of CoPc molecules on pure metal surfaces, both the LUMO of the macrocycle and Co 3d unoccupied orbitals can be hybridized with substrate states or be filled by charge transfer from the substrate since their energies are very close.[58,62,66] Very recently, some theoretical results show that the proper selection of the functionals is very important for the better description of the d orbitals of the transition metal ion center of MPc.[64,65] In the current study, we chose the spin-polarized GGA of Perdew and Wang (PW91)[70] for the exchange-correlation energy, which should have a similar accuracy to the PBE.[65] However, we are only aware of a few studies for CoPc on R3-Ag/Si surface.[39,71,72] A direct comparison of our results with others is currently not available. We noted that the calculations for the thick films of MPc are much better than that for the thin films (monolayer),[59] which may be attributed to the weakened interaction of the topmost molecules with the metal substrates. We expect a weaker interaction for the CoPc with the R3-Ag/Si substrate than those for the MPc with the pure metal substrates. The relatively low adsorption energies and the bias-dependent PDOS from our calculations can well support this idea, even though the self-interaction errors[73−76] can still be a drawback in the determination of the exact electronic states of the CoPc for the calculation method used in this study. On the basis of our experimental observations and analysis above, we believe that the d_{z^2} orbital should be above but not too far away from the Fermi energy, and the mechanism proposed here still holds.

Role of the SCL. By varying the tunneling conditions of set point current or bias voltage, it mainly causes the width change of the tip−molecule gap, as a result, leading to the redistribution of the voltage drops at every junction. In Figure 3e, it shows a broadened width of the tip−molecule gap. In this case, for $V_{inter} \approx$ 0.1 V, the V_{gap}/V fraction becomes larger, and the V_{SCL}/V fraction becomes smaller, while the total applied voltage decreases. This may lead to the alignment of the d_{z^2} orbital of the Co^{2+} ion with the SS band S_1 at a smaller applied bias voltage, consequently resulting in the shift of the NDR position toward the Fermi level. As we will discuss below, this situation is sensitively affected by the width of the SCL, which may cause the variation of the voltage drop at the SCL.

At 80 K, the width of the SCL even in the lightly doped *n*-type wafer can be relatively thin,[51] so that the voltage drop at the SCL, V_{SCL}, is relatively small. If we simply neglect the effect of the SCL, we can get an estimated V_{gap}/V_{inter} ratio of about 10 according to the observed NDR peak position of −1.1 V (Figure 1b) when the resonance occurs under the voltage drop of $V_{inter} \approx$ 0.1 V (Figure 3b). The fraction V_{inter}/V is reasonably estimated to be less than 10%. It is noted that the NDR obtained at the Co^{2+} ion center in sample no. 2 (lightly doped *p*-type Si) occurs at around −1.1 V, similar to that in sample no. 1 (lightly doped *n*-type Si). It indicates that the fractions V_{SCL}/V in these two samples are small at 80 K, and the dominant voltage drop is still at the vacuum gap. This makes the small difference in the NDR positions in these two samples, even though the SCL width in sample no. 2 is estimated to be narrower by about 1 order of magnitude than that in sample no. 1.[77,78] As a comparison, the NDR occurs at around −0.75 V in sample no. 3 (heavily doped *n*-type Si) because of its much narrower SCL by 2 orders of magnitude than that in sample no. 1.

The independence of NDR on the doping type can be understood in our model on the basis of the electronic nature of R3-Ag/Si surface that the surface-states of R3-Ag/Si is irrespective of doping type and concentration in the bulk.[42−50] Since the d_{z^2} orbital of Co^{2+} ion is located above the E_F, it can only align with the S_1 under a negative bias voltage irrespective of doping type of the Si substrate (Figure 3, and see Supporting Information).

The appearance of NDR at Co^{2+} ion centers is independent of the adsorption sites and the molecular orientations of CoPc molecules (Figure 1c), quite different from the behaviors of the site-dependent NDR on the bare R3-Ag/Si surface where the NDR is only observed at the inequivalent triangles of Ag atoms.[51] This fact can also be explained by considering the different electronic properties of the S_1 and the S_2/S_3 states. In the bare R3-Ag/Si surface, the occurrence of NDR is strongly dependent on the measuring temperature and the doping concentration, as well as the specific sites.[51] At a low temperature of 5 K and with a lightly doped Si wafer, the SCL can be wide enough to limit tunneling rate between the S_2/S_3 and the bulk states.[51] This is something similar to the mechanism of the B dopant on a silicon surface.[79] Unlike the strongly localized S_2/S_3 states at the Ag triangles, the S_1 state is much dispersive and thus has an extended wave function.[43,45,46] As we discussed above, the independence of the NDR on the CoPc adsorption sites is thus understandable, since the NDR originates from the resonance between the d_{z^2} orbital of Co^{2+} ion and the spatially extended S_1 state.

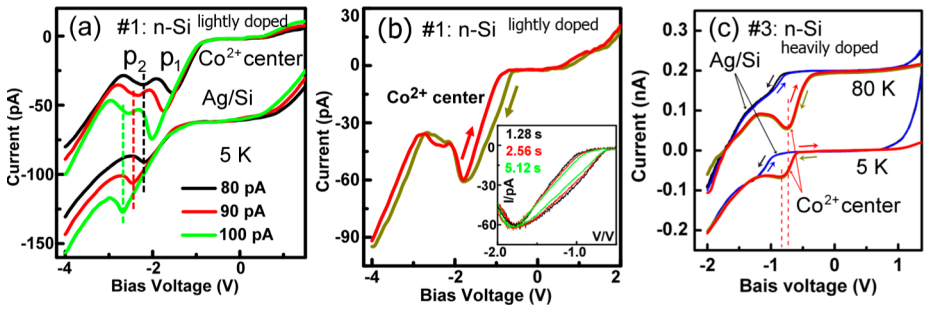

Figure 4. (a) *I*−*V* curves measured at the Co^{2+} ion center of a CoPc molecule and the Ag triangle of R3-Ag/Si surface in sample no. 1 (set point: −4.0 V and 80, 90, and 100 pA) at 5 K. The NDR peaks at lower and higher negative bias voltages in the curves measured at the Co^{2+} ion center are denoted as p_1 and p_2, respectively, where p_2 correspondingly locates almost at the same NDR positions of the bare R3-Ag/Si surface, as marked by the dashed lines. (b) *I*−*V* curves taken at the Co^{2+} ion center in a cycle of forward and backward voltage sweeping at 5 K. (set point: −4.0 V and 90 pA). Inset: forward and backward *I*−*V* curves measured at different acquisition time of 1.3 s (black), 2.6 s (red), and 5.1 s (green). (c) Typical *I*−*V* curves taken at Co^{2+} ion center and at R3-Ag/Si surface in sample no. 3 at 80 and 5 K (−2.0 V and 200 pA), respectively. The curves recorded at each site in forward and backward sweeping cycle are almost completely overlapped, showing no hysteresis in sample no. 3 both at 80 and 5 K. The *I*−*V* curves taken at 80 K are shifted upward for clarity.

Dependence of NDR Position on Doping Concentration of the Si Substrate at 5 K. *Measurement of NDR at 5 K.* As a further confirmation, we show the NDR behaviors at the Co^{2+} ion center of the CoPc on the R3-Ag/Si surface with a lightly doped *n*-type Si wafer (sample no. 1) measured at 5 K, as shown in Figure 4a. It is observed that there are two NDR peaks in each *I*−*V* curve. The NDR peak at the higher negative bias (denoted as p_2) correspondingly locates at almost the same NDR voltage of the bare R3-Ag/Si surface, as marked by the dashed lines for the *I*−*V* curves with different measuring conditions, respectively. We may attribute p_2 to the similar origination due to the contribution of the localized S_2/S_3 states, since it also shows the similar site-dependent behavior as the bare R3-Ag/Si surface.[51] We may thus assign the NDR peak at the lower negative bias (denoted as p_1) to the mechanism of the resonance between the d_{z^2} orbital of Co^{2+} ion and the spatially extended S_1 state, as we discussed above.

Aspects of the Different Contributions of the Band S_1 and the Bands S_2/S_3. According to the energy diagram (Figure 3), only at a relatively higher bias voltage can the E_F of the STM tip sweep the SS band S_2/S_3,[51] causing p_2 to locate at a higher bias voltage than p_1. This result obtained at 5 K is consistent with the results measured at 80 K; that is, the shoulder feature locates at a higher voltage than the NDR (Figure 1c,d). It is observed that the NDR ratio of p_2 is much less pronounced than that of p_1, moreover, the NDR peak of p_2 can become almost invisible when the CoPc molecule is centered offset of the Ag triangles or on the hole sites of R3-Ag/Si surface, while the p_1 is not affected. Their different behaviors of these two NDR peaks reflect their different mechanisms.

Effect of the SCL at 5 K. Compared to the results obtained at 80 K, the NDR positions in sample no. 1 are no longer slightly dependent on the measuring conditions at 5 K and the NDR positions shift to relatively high negative bias voltages. This fact can be assigned to a large fraction of the voltage drop at the SCL, because the SCL has a much lower carrier concentration and thus becomes much wider at 5 K.[51] In this case, the NDR positions of p_2 (p_1) vary significantly from −2.6 to −2.2 V (−2.0 to −1.5 V) with the set point current decreasing from 100 to 80 pA, as shown in Figure 4a. Decreasing the set point current at the same bias voltage actually increases the distance of the vacuum gap between the tip and the sample, thus increasing the voltage drops of V_{gap} and V_{inter}, and decreasing the one of V_{SCL} (Figure 3c). This leads to the alignment of the d_{z^2} orbital of Co^{2+} ion with the SS band S_1, as well as the alignment of the E_F of the tip with the SS band S_2/S_3 at smaller applied bias voltages, consequently resulting in the shift toward the Fermi level for both of the NDR peaks (Figure 4a). In sample no. 1 with the lightly doped *n*-type Si wafer at 5 K, we also observed the hysteresis in the *I*−*V* curves, as shown in Figure 4b. Moreover, the magnitude of the hysteresis shows dependence on the acquisition time of the *I*−*V* curves; that is, the longer acquisition time gives a smaller hysteresis, which confirms the role of the relatively wide SCL because of the charging process, similar to the observations in the bare R3-Ag/Si surface.[51]

NDR Behaviors in the Sample with a Heavily Doped Si Substrate. Differently, in sample no. 3 with a heavily doped Si substrate, the NDR position of the Co^{2+} ion center just varies in the small range of −0.75 to −0.90 V with the change of measuring temperature from 80 to 5 K, as shown in Figure 4c. Along with only the shoulder feature occurring in the *I*−*V* curves taken at the bare Ag/Si surface, there is only one NDR peak in the *I*−*V* curves taken at the Co^{2+} ion center. No obvious hysteresis can be observed yet in sample no. 3 at 5 K. This behavior is attributed to the relatively thin SCL in sample no. 3, as compared to those in samples no. 1 and no. 2 at 80 K (Figure 1d). Therefore, the NDR

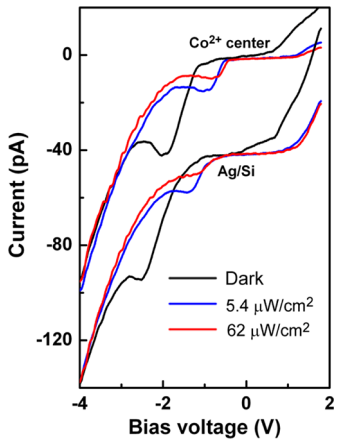

Figure 5. $I-V$ curves measured at the Co^{2+} ion center of a CoPc molecule in comparison with the ones at the Ag triangle of R3-Ag/Si surface (−4.0 V and 100 pA) under illumination with various light intensities. The curves measured at R3-Ag/Si surface are shifted downward for clarity. All $I-V$ curves are obtained at 5 K.

position is dominantly determined by the voltage drops of V_{gap} and V_{inter}. Once V_{inter} = 0.1 V, the NDR occurs due to the alignment of the d_{z^2} orbital of the Co^{2+} ion with the S_1 band. In this case, the relatively thin SCL just slightly affects the NDR position.

It is noted that the widths of NDR at 5 K are wider than the ones at 80 K (compare Figure 4a with Figure 1c). This feature actually validates our model present in Figure 3 in another way. In the current study, the CoPc molecules are put in the middle of the double barrier tunneling junction: tip-molecule and molecule−substrate. On the basis of our model in Figure 3, the voltage sweeping between the tip and the sample may not directly reflect the sweeping between the d_{z^2} orbital and the S_1 states. For sample no. 1 at 80 K, the sweeping between the d_{z^2} orbital and the S_1 state is dependent on the fraction V_{inter}/V [$=V_{inter}/(V_{inter} + V_{gap})$] if the SCL is negligible. At 5 K, because the SCL cannot be neglected, there is a much smaller fraction V_{inter}/V [$=V_{inter}/(V_{inter} + V_{gap} + V_{SCL})$] at the molecule−substrate interface. In this case, the d_{z^2} orbital can sweep the S_1 states more "slowly" while the total voltage V may already sweep a quite wide range. Therefore, the recorded NDR width (the range according to V) at 80 K is sharper than that at 5 K in sample no. 1. However, in the case of sample no. 3, when the SCL is not the significant factor both at 80 and 5 K, the NDR width may show in a similar level (Figure 4c).

Tuning the NDR Position with Light Illumination. The NDR position can be tuned by light illumination for CoPc molecules on R3-Ag/Si surface (sample no. 1) at 5 K. In our experiment, the sample was illuminated with a mercury−xenon lamp (Hamamatsu, L2423) *in situ* at 5 K. A band-pass filter centered at 532 nm and bandwidth of 50 nm was used. Figure 5 shows the $I-V$ curves measured at the center of the CoPc molecule and at the Ag triangles of the R3-Ag/Si surface with various light intensity: dark, 5.4 $\mu W/cm^2$, 62 $\mu W/cm^2$, respectively. The NDR position shifts toward the Fermi level with the increase of the light intensity. It is noticed that the NDR position obtained at the CoPc center shifts to −0.8 V under the illumination with the light intensity of 62 $\mu W/cm^2$ at 5 K, which is nearly at the same position as the one for the Co^{2+} ion of CoPc on the R3-Ag/Si surface in sample no. 3 with the heavily doped *n*-type Si wafer at 80 K. The NDR position obtained at the Ag triangles of R3-Ag/Si surface is more negative than that obtained at the Co^{2+} ion center, even though this peak is not obviously visible in the $I-V$ curves taken at the Co^{2+} center (Figure 5). The shift of the NDR position under light illumination can be understood by taking the width change of the SCL into consideration. Under light illumination at 5 K, the electrons in the valence band of Si can be excited to the conduction band, causing a higher carrier density in the bulk, which can be comparable with that in the heavily doped wafer at 80 K. As a result, the SCL width even at 5 K can be decreased under the light illumination, even to the similar level in the heavily doped Si substrate at 80 K, making the NDR at 5 K almost behave like the one for CoPc on the R3-Ag/Si surface with the heavily doped *n*-type wafer at 80 K. Our measurements were performed only after the thermal equilibrium was reached, and the thermal change upon illumination could be neglected.

It is known that the conductance of lightly doped Si is much low at 5 K.[3] One may concern that the conducting channel can be just provided by the Ag overlayer, but not the Si substrate. To exclude this possibility, we measured the bare Si(111)-7 × 7 substrate before Ag deposition (lightly doped *n*-type Si for sample no. 1). We could only image the Si surface by applying relatively high bias voltages higher than ±4 V under a relatively low set point current of several tens pA. This means that the Si substrate can still be the conducting channel. The value of the available bias voltage is consistent with measurement conditions used in the R3-Ag/Si sample. Moreover, the tuning effect under the light illumination with various intensities also confirms that the band structure of the Si substrate plays an important role in the electron transport, in which the carriers excited by the photons cause the narrowed SCL and tune the NDR position systematically. This phenomenon may well support our model.

Advantages of Using the Intrinsic Surface State of R3-Ag/Si Surface. The NDR has been widely studied in various molecular systems. Different mechanisms have been revealed, such as the resonance between either intermolecular levels[56,80−82] or intramolecular levels,[83] the conformational changes of molecules excited by the inelastic tunneling electrons,[84−89] the symmetry matching between specific molecular orbitals and

the electrode,[90] the presence of molecules in a double barrier tunnel junction,[91] and voltage-driven and high-electric-field induced soft breakdown in the SiO_x layer on Si.[92,93] Since in such systems the NDR is not directly related to the property of semiconductors, it needs to be further designed for compatibility with the existing silicon-based technology. Our finding here demonstrates that one can directly make use of the resonance between the intrinsic surface states of R3-Ag/Si surface and molecular orbital to produce the robust NDR.

There are several advantages to building molecular NDR devices by making use of the intrinsic surface-states of a passivated silicon surface. First, since the molecules are weakly physisorbed on the surface, it is possible to form functional molecular device patterns on the surface through the molecular self-assembly method.[37−40] Second, the appearance of the NDR effect at the molecule does not depend on the doping type and doping concentration of the silicon substrate, giving more flexibility to the selection of silicon substrate. Moreover, the light illumination experiment demonstrates that it is possible to build light-sensitive molecular NDR devices based on this hybrid silicon-molecular system.

CONCLUSIONS

We have studied the electron transport behaviors of single CoPc molecules on the R3-Ag/Si surface using STM measured at 5 and 80 K. The CoPc molecule shows an NDR effect at its center, irrespective of measuring temperature and doping type and doping concentration of the silicon substrate. On the basis of our DFT calculations, the NDR observed at the CoPc center is attributed to the resonant tunneling between the SS band S_1 and the localized d_{z^2} orbital of the central Co^{2+} ion. In comparison, H_2Pc molecules on R3-Ag/Si do not produce NDR because they lack a similar molecular orbital near the Fermi level. The NDR position of the Co^{2+} ion center of CoPc on the R3-Ag/Si surface (with light-doped silicon substrate) locates at a much high negative bias voltage at 5 K, which is explained by considering the voltage drop at the SCL. It is found that the NDR position can be tuned through light illumination with various light intensities. By taking advantage of the intrinsic surface-states of the R3-Ag/Si surface and the proper molecular orbital of the CoPc molecule, we demonstrate a way to build a single-molecular NDR device on silicon, which may be used to fabricate hybrid silicon−molecular electronics.

METHODS

Our experiments were carried out using an ultrahigh vacuum low-temperature scanning tunneling microscope (Omicron) with a base pressure of 3×10^{-11} Torr. The Si(111)-7 × 7 surface was prepared by degassing the Si(111) substrate at 873 K for about 10 h, then flashing to 1500 K for several times, rapidly cooling down to 1200 K, and slowly cooling down to room temperature. The R3-Ag/Si surface was obtained by depositing 1 ML Ag onto the Si(111)-7 × 7 surface at about 650 K and annealing at the same temperature for 20 min. Three different Si(111) wafers were used: lightly doped *n*-type wafer (P doped with concentration of 5×10^{14} cm^{-3}), heavily doped *n*-type wafer (P doped with concentration of 1×10^{18} cm^{-3}), and *p*-type wafer (B doped with concentration of 5×10^{15} cm^{-3}). CoPc molecules were deposited onto the clean R3-Ag/Si surfaces held at room temperature. For comparison, H_2Pc was also measured. The presented data were acquired at 80 or 5 K. Electrochemically etched tungsten tips were used, which had been subjected to careful cleaning treatments.

The electronic structures of the adsorbed CoPc and H_2Pc on the R3-Ag/Si surface were calculated using density functional theory. All calculations were performed using the Vienna *ab initio* simulation package (VASP)[94] within the spin-polarized GGA of Perdew and Wang[70] for the exchange-correlation energy. A plane-wave basis set with cutoff energy of 384 eV for the valence electron state and the Vanderbilt ultrasoft pesudopotentials[95] for the core−electron interactions were employed. The optimized lattice constant of Si is 5.458 Å. The inequivalent-triangle (IET)[43,48,52−54] structure of R3-Ag/Si was described by a slab consisting of a silver layer, a missing top Si layer, three Si double layers, and a vacuum layer of 10 Å. A hydrogen layer was added to saturate the Si dangling bonds at the bottom surface. During the optimization of the slab, 8 × 8 × 1 Monk-horst[96] mesh of *k* points were used, and all atoms except the bottom Si double layer and the hydrogen atoms were allowed to relax until the forces on atoms were smaller than 0.02 eV/Å. A CoPc (or H_2Pc) molecule was then put onto a 3 × 3 (relative to the $\sqrt{3} \times \sqrt{3}$ unit cell) supercell. The structure was again optimized with a bottom Si double layer and the hydrogen layer fixed until all forces on atoms were smaller than 0.02 eV/Å. Several configurations were calculated, such as putting the center of the molecule on the top of a Ag atom, at the center of a small Ag triangle, at the center of large Ag triangle, at the bridge site between two Ag atoms, and at the hollow site. In all of these configurations, the molecular orientation was adopted from the experimental observations; that is, one of the symmetric axes of the molecule tilting by 15° with respect to the $\langle 11\bar{2} \rangle$ directions of the R3-Ag/Si surface. The distance between the R3-Ag/Si surface and the molecule is about 3 Å. Owing to the numerical limitations, only the Γ point was used for the calculation of the molecule/substrate system.

Conflict of Interest: The authors declare no competing financial interest.

Acknowledgment. This work was supported by NBRP (Grant 2011CB921400) and NSFC (Grants 9021013, 10825415, 10874164), China.

Supporting Information Available: Orientations of CoPc molecules adsorbed on R3-Ag/Si surface; H_2Pc molecules on the R3-Ag/Si surface; energy diagram in the case of *p*-type Si substrate; and PDOS of the Co^{2+} ion center with various adsorption sites on R3-Ag/Si. This material is available free of charge *via* the Internet at http://pubs.acs.org.

REFERENCES AND NOTES

1. Joachim, C.; Gimzewski, J. K.; Aviram, A. Electronics Using Hybrid-Molecular and Mono-Molecular Devices. *Nature* **2000**, *408*, 541–548.
2. McCreery, R. L. Molecular Electronic Junctions. *Chem. Mater.* **2004**, *16*, 4477–4496.
3. Richard, L.; McCreery, R. L.; Bergren, A. J. Progress with Molecular Electronic Junctions: Meeting Experimental

Challenges in Design and Fabrication. *Adv. Mater.* **2009**, *21*, 4303–4322.
4. Metzger, R. M. Unimolecular Electronics. *J. Mater. Chem.* **2008**, *18*, 4364–4396.
5. Heath, J. R. Molecular Electronics. *Annu. Rev. Mater. Res.* **2009**, *39*, 1–23.
6. Moth-Poulsen, K.; Bjørnholm, T. Molecular Electronics with Single Molecules in Solid-State Devices. *Nat. Nanotechnol.* **2009**, *4*, 551–556.
7. Pan, S.; Zhao, A. D.; Wang, B.; Yang, J. L.; Hou, J. G. Controlling Electronic States and Transport Properties at the Level of Single Molecules. *Adv. Mater.* **2010**, *22*, 1967–1971.
8. Cerofolini, G. F.; Arena, G.; Camalleri, C. M.; Galati, C.; Reina, S.; Renna, L.; Mascolo, D. A Hybrid Approach to Nanoelectronics. *Nanotechology* **2005**, *16*, 1040–1047.
9. Aswal, D. K.; Lenfant, S.; Guerin, D.; Yakhmi, J. V.; Vuillaume, D. Self Assembled Monolayers on Silicon for Molecular Electronics. *Anal. Chim. Acta* **2006**, *568*, 84–108.
10. Vilan, A.; Yaffe, O.; Biller, A.; Salomon, A.; Kahn, A.; Cahen, D. Molecules on Si: Electronics with Chemistry. *Adv. Mater.* **2010**, *22*, 140–159.
11. Vuillaume, D. Molecular Nanoelectronics. *Proc. IEEE* **2010**, *98*, 2111–2123.
12. Hersam, M. C.; Guisinger, N. P.; Lyding, J. W. Silicon-Based Molecular Nanotechnology. *Nanotechnology* **2000**, *11*, 70–76.
13. Aswal, D. K.; Koiry, S. P.; Jousselme, B.; Gupta, S. K.; Palacin, S.; Yakhmi, J. V. Hybrid Molecule-on-Silicon Nanoelectronics: Electrochemical Processes for Grafting and Printing of Monolayers. *Phys. E* **2009**, *41*, 325–344.
14. Gergel-Hackett, N.; Zangmeister, C. D.; Hacker, C. A.; Richter, L. J.; Richter, C. A. Demonstration of Molecular Assembly on Si (100) for CMOS-Compatible Molecule-Based Electronic Devices. *J. Am. Chem. Soc.* **2008**, *130*, 4259–4261.
15. Sze, S. M. *Semiconductor Devices: Physics and Technology*; John Wiley & Sons: New York, 2002.
16. Lu, P. H.; Polanyi, J. C.; Rogers, D. Photoinduced Localized Atomic Reaction (LAR) of 1,2- and 1,4-Dichlorobenzene with Si(111) 7 × 7. *J. Chem. Phys.* **2000**, *112*, 11005–11010.
17. McNab, I. R.; Polanyi, J. C. Patterned Atomic Reaction at Surfaces. *Chem. Rev.* **2006**, *106*, 4321–4354.
18. Hossain, M. Z.; Kato, H. S.; Kawai, M. Self-Directed Chain Reaction by Small Ketones with the Dangling Bond Site on the Si(100)-(2 × 1)-H Surface: Acetophenone, a Unique Example. *J. Am. Chem. Soc.* **2008**, *130*, 11518–11523.
19. Lopinski, G. P.; Wayner, D. D. M.; Wolkow, R. A. Self-Directed Growth of Molecular Nanostructures on Silicon. *Nature* **2000**, *406*, 48–51.
20. Hamers, R. J.; Coulter, S. K.; Ellison, M. D.; Hovis, J. S.; Padowitz, D. F.; Schartz, M. P.; Greenlief, C. M.; Russel, J. N. Cycloaddition Chemistry of Organic Molecules with Semiconductor Surfaces. *Acc. Chem. Res.* **2000**, *33*, 617–624.
21. Hurley, P. T.; Nemanick, E. J.; Brunschwig, B. S.; Lewis, N. S. Covalent Attachment of Acetylene and Methylacetylene Functionality to the Si(111) Surfaces: Scaffolds for Organic Surface Functionalization while Retaining Si−C Passivation of Si(111) Surface Sites. *J. Am. Chem. Soc.* **2006**, *128*, 9990–9991.
22. Garah, M. E.; Makoudi, Y.; Duverger, É.; Palmino, F.; Rochefort, A.; Chérioux, F. Large-Scale Patterning of Zwitterionic Molecules on a Si(111)-7 × 7 Surface. *ACS Nano* **2011**, *5*, 424–428.
23. Guisinger, N. P.; Greene, M. E.; Basu, R.; Baluch, A. S.; Hersam, M. C. Room Temperature Negative Differential Resistance through Individual Organic Molecules on Silicon Surfaces. *Nano Lett.* **2004**, *4*, 55–59.
24. Guisinger, N. P.; Yoder, N. L.; Hersam, M. C. Probing Charge Transport at the Single-Molecule Level on Silicon by Using Cryogenic Ultrahigh Vacuum Scanning Tunneling Microscopy. *Proc. Natl. Acad. Sci. U.S.A.* **2005**, *102*, 8838–8343.
25. Hallbäck, A.-S.; Poelsema., B; Zandvliet, H. J. W. Negative Differential Resistance of TEMPO Molecules on Si(111). *Appl. Surf. Sci.* **2007**, *253*, 4066–4071.
26. Rakshit, T.; Liang, G.-C.; Ghosh, A. W.; Datta, S. Silicon-Based Molecular Electronics. *Nano Lett.* **2004**, *4*, 1803–1807.
27. Quek, S. Y.; Neaton, J. B.; Hybertsen, M. S.; Kaxiras, E.; Louie, S. G. Negative Differential Resistance in Transport through Organic Molecules on Silicon. *Phys. Rev. Lett.* **2007**, *98*, 066807.
28. Schofield, S. R.; Saraireh, S. A.; Smith, P. V.; Radny, M. W.; King, B. V. Organic Bonding to Silicon *via* a Carbonyl Group: New Insights from Atomic-Scale Images. *J. Am. Chem. Soc.* **2007**, *129*, 11402–11407.
29. Nicoara, N.; Paz, Ó.; Méndez, J.; Baró, A. M.; Soler, J. M.; Gómez-Rodríguez, J. M. Adsorption and Electronic Properties of PTCDA Molecules on Si(111)-(7 × 7): Scanning Tunneling Microscopy and First-Principles Calculations. *Phys. Rev. B* **2010**, *82*, 075402.
30. Lo, R. -L.; Chang, C. -M.; Hwang, I. -S.; Tsong, T. T. Observation of Single Oxygen Atoms Decomposed from Water Molecules on a Si(111)-7 × 7 Surface. *Phys. Rev. B* **2006**, *73*, 075427.
31. Yoder, N. L.; Fakonas, J. S.; Hersam; Mark, C. Control and Characterization of Cyclopentene Unimolecular Dissociation on Si(100) with Scanning Tunneling Microscopy. *J. Am. Chem. Soc.* **2009**, *131*, 10059–10065.
32. Bellec, A.; Ample, F.; Riedel, D.; Dujardin, G.; Joachim, C. Imaging Molecular Orbitals by Scanning Tunneling Microscopy on a Passivated Semiconductor. *Nano Lett.* **2009**, *9*, 144–147.
33. Baris, B.; Luzet, V.; Duverger, E.; Sonnet, P.; Palmino, F.; Cherioux, F. Robust and Open Tailored Supramolecular Networks Controlled by the Template Effect of a Silicon Surface. *Angew. Chem., Int. Ed.* **2011**, *50*, 4094–4098.
34. Wang, K. D.; Zhao, J.; Yang, S. F.; Chen, L.; Li, Q. X.; Wang, B.; Yang, S. H.; Yang, J. L.; Hou, J. G.; Zhu, Q. S. Unveiling Metal-Cage Hybrid States in a Single Endohedral Metallofullerene. *Phys. Rev. Lett.* **2003**, *91*, 185504.
35. Li, Q.; Yamazaki, S.; Eguchi, T.; Kim, H.; Kahng, S. -J.; Jia, J. F.; Xue, Q. K.; Hasegawa, Y. Direct Evidence of the Contribution of Surface States to the Kondo Resonance. *Phys. Rev. B* **2009**, *80*, 115431.
36. Li, Q.; Yamazaki, S.; Eguchi, T.; Kim, H.; Kahng, S.-J.; Jia, J.-F.; Xue, Q.-K.; Hasegawa, Y. Initial Adsorption and Kondo Resonance of 5,10,15,20-Tetrakis(4-bromophenyl)porphyrin−Co Molecules on Ag/Si(111) Surface Studied by Low-Temperature Scanning Tunneling Microscopy/Spectroscopy. *Jpn. J. Appl. Phys.* **2009**, *48*, 08JB01.
37. Zhang, H. M.; Gustafsson, J. B.; Johansson, L. S. O. STM Study of the Electronic Structure of PTCDA on Ag/Si(111)-$\sqrt{3}\times\sqrt{3}$. *Chem. Phys. Lett.* **2010**, *485*, 69–76.
38. Beggan, J. P.; Krasnikov, S. A.; Sergeeva, N. N.; Senge, M. O.; Cafolla, A. A. Self-Assembly of Ni(II) Porphine Molecules on the Ag/Si(111)-($\sqrt{3}\times\sqrt{3}$)R30° Surface Studied by STM/STS and LEED. *J. Phys.: Condens. Matter* **2008**, *20*, 015003.
39. Upward, M. D.; Beton, P. H.; Moriarty, P. Adsorption of Cobalt Phthalocyanine on Ag Terminated Si(111). *Surf. Sci.* **1999**, *441*, 21–25.
40. Theobald, J. A.; Oxtoby, N. S.; Phillips, M. A.; Champness, N. R.; Beton, P. H. Controlling Molecular Deposition and Layer Structure with Supramolecular Surface Assemblies. *Nature* **2003**, *424*, 1029–1031.
41. He, T.; Ding, H. J.; Peor, N.; Lu, M.; Corley, D. A.; Chen, B.; Ofir, Y.; Gao, Y. L.; Yitzchaik, S.; Tour, J. M. Silicon/Molecule Interfacial Electronic Modifications. *J. Am. Chem. Soc.* **2008**, *130*, 1699–1710.
42. Hasegawa, S.; Tong, X.; Takeda, S.; Sato, N.; Nagao, T. Structures and Electronic Transport on Silicon Surfaces. *Prog. Surf. Sci.* **1999**, *60*, 89–257.
43. Chen, L.; Xiang, H. J.; Li, B.; Zhao, A.; Xiao, X.; Yang, J.; Hou, J. G.; Zhu, Q. Detecting Surface Resonance States of Si-(111)-$\sqrt{3}\times\sqrt{3}$-Ag with a Scanning Tunneling Microscope. *Phys. Rev. B* **2004**, *70*, 245431.
44. Johansson, L. S. O.; Landemark, E.; Karlsson, C.; Uhrberg, R. Fermi-Level Pinning and Surface-State Band Structure of the Si(111)-($\sqrt{3}\times\sqrt{3}$)R30°-Ag Surface. *Phys. Rev. Lett.* **1989**, *63*, 2092–2095.

45. Tong, X.; Jiang, C. S.; Hasegawa, S. Electronic Structure of the Si(111)-$\sqrt{21}\times\sqrt{21}$-(Ag+Au) Surface. *Phys. Rev. B* **1998**, *57*, 9015–9023.
46. Tong, X.; Ohuchi, S.; Sato, N.; Tanikawa, T.; Nagao, T.; Matsuda, I.; Aoyagi, Y.; Hasegawa, S. Electronic Structure of Ag-Induced $\sqrt{3}\times\sqrt{3}$ and $\sqrt{21}\times\sqrt{21}$ Superstructures on the Si(111) Surface Studied by Angle-Resolved Photoemission Spectroscopy and Scanning Tunneling Microscopy. *Phys. Rev. B* **2001**, *64*, 205316.
47. Yokotsuka, T.; Kono, S.; Suzuki, S.; Sagawa, T. Study of Ag/Si(111) Submonolayer Interface: I. Electronic Structure by Angle-Resolved UPS. *Surf. Sci.* **1983**, *127*, 35–47.
48. Aizawa, H.; Tsukada, M.; Sato, N.; Hasegawa, S. Asymmetric Structure of the Si(111)- $\sqrt{3}\times\sqrt{3}$-Ag Surface. *Surf. Sci.* **1999**, *429*, L509–L514.
49. Ono, M.; Nishigata, Y.; Nishio, T.; Eguchi, T.; Hasegawa, Y. Electrostatic Potential Screened by a Two-Dimensional Electron System: A Real-Space Observation by Scanning-Tunneling Spectroscopy. *Phys. Rev. Lett.* **2006**, *96*, 016801.
50. Viernow, J.; Henzler, M.; O'Brien, W. L.; Men, F. K.; Leibsle, F. M.; Petrovykh, D. Y.; Lin, J. L.; Himpsel, F. J. Unoccupied Surface States on Si(111)$\sqrt{3}\times\sqrt{3}$-Ag. *Phys. Rev. B* **1998**, *57*, 2321–2326.
51. Wang, W. H.; Zhao, A. D.; Wang, B.; Hou, J. G. Probing Negative Differential Resistance on Si(111)-$\sqrt{3}\times\sqrt{3}$-Ag Surface with Scanning Tunneling Microscopy. *Appl. Phys. Lett.* **2009**, *94*, 262108.
52. Sato, N.; Nagao, T.; Hasegawa, S. Si(111)-($\sqrt{3}\times\sqrt{3}$)-Ag Surface at Low Temperatures: Symmetry Breaking and Surface Twin Boundaries. *Surf. Sci.* **1999**, *442*, 65–73.
53. Zhang, H. M.; Uhrberg, R. I. G. Ag/Si(111)$\sqrt{3}\times\sqrt{3}$: Surface Band Splitting and the Inequivalent Triangle Model. *Phys. Rev. B* **2006**, *74*, 195329.
54. Jeong, H.; Yeom, H. W.; Jeong, S. Adatom-Induced Variations of the Atomic and Electronic Structures of Si(111)$\sqrt{3}\times\sqrt{3}$-Ag: A First-Principles Study. *Phys. Rev. B* **2008**, *77*, 235425.
55. Lyo, I.-W.; Avouris, P. Negative Differential Resistance on the Atomic Scale: Implications for Atomic Scale Devices. *Science* **1989**, *245*, 1369–1371.
56. Zeng, C.; Wang, H. Q.; Wang, B.; Yang, J. L.; Hou, J. G. Negative Differential-Resistance Device Involving Two C_{60} Molecules. *Appl. Phys. Lett.* **2000**, *77*, 3595–3597.
57. Takada, M.; Tada, H. Direct Observation of Adsorption-Induced Electronic States by Low-Temperature Scanning Tunneling Microscopy. *Ultramicroscopy* **2005**, *105*, 22–25.
58. Annese, E.; Fujii, J.; Vobornik, I.; Rossi, G. Structure and Electron States of Co−Phthalocyanine Interacting with the Cu(111) Surface. *J. Phys. Chem. C* **2011**, *115*, 17409–17416.
59. Xiao, J.; Dowben, P. A. The Role of the Interface in the Electronic Structure of Adsorbed Metal(II) (Co, Ni, Cu) Phthalocyanines. *J. Mater. Chem.* **2009**, *19*, 2172–2178.
60. Hill, I. G.; Kahn, A.; Soos, Z. G.; Pascal, R. A., Jr. Charge-Separation Energy in Films of π-Conjugated Organic Molecules. *Chem. Phys. Lett.* **2000**, *327*, 181–188.
61. Lu, X.; Hipps, K. W.; Wang, X. D.; Mazur, U. Scanning Tunneling Microscopy of Metal Phthalocyanines: d_7 and d_9 Cases. *J. Am. Chem. Soc.* **1996**, *118*, 7197–7202.
62. Stadtmüller, B.; Kröger, I.; Reinert, F.; Kumpf, C. Submonolayer Growth of CuPc on Noble Metal Surfaces. *Phys. Rev. B* **2011**, *83*, 085416(10 pages).
63. Reynolds, P. A.; Figgis, B. N. Metal Phthalocyanine Ground States: Covalence and *ab Initio* Calculation of Spin and Charge Densities. *Inorg. Chem.* **1991**, *30*, 2294–2300.
64. Marom, N.; Ren, X. G.; Moussa, J. E.; Chelikowsky, J. R.; Kronik, L. Electronic Structure of Copper Phthalocyanine from G_0W_0 Calculations. *Phys. Rev. B* **2011**, *84*, 195143.
65. Zhang, Y. Y.; Du, S. X.; Gao, H.-J. Binding Configuration, Electronic Structure, and Magnetic Properties of Metal Phthalocyanines on a Au(111) Surface Studied with *ab Initio* Calculations. *Phys. Rev. B.* **2011**, *84*, 125446.
66. Baran, J. D.; Larsson, J. A.; Woolley, R. A. J.; Cong, Y.; Moriarty, P. J.; Cafolla, A. A.; Schulte, K.; Dhanak, V. R. Theoretical and Experimental Comparison of SnPc, PbPc, and CoPc Adsorption on Ag(111). *Phys. Rev. B* **2010**, *81*, 075413.
67. Perdew, J. P.; Burke, K.; Ernzerhof, M. Generalized Gradient Approximation Made Simple. *Phys. Rev. Lett.* **1996**, *77*, 3865–3868; **1997**, *78*, 1396–1396.
68. Kümmel, S.; Kronik, L. Orbital-Dependent Density Functionals: Theory and Applications. *Rev. Mod. Phys.* **2008**, *80*, 3–60.
69. Stowasser, R.; Hoffmann, R. What Do the Kohn−Sham Orbitals and Eigenvalues Mean?. *J. Am. Chem. Soc.* **1999**, *121*, 3414–3420.
70. Perdew, J. P.; Wang, Y. Accurate and Simple Analytic Representation of the Electron−Gas Correlation Energy. *Phys. Rev. B* **1992**, *45*, 13244–13249.
71. Song, F.; Wells, J. W.; Handrup, K.; Li, Z. S.; Bao, S. N.; Schulte, K.; Ahola-Tuomi, M.; Mayor, L. C.; Swarbrick, J. C.; Perkins, E. W.; *et al*. Direct Measurement of Electrical Conductance through a Self-Assembled Molecular Layer. *Nat. Nanotechnol.* **2009**, *4*, 373–376.
72. Song, F.; Gammelgaard, L.; Hofmann, Ph.; Wells, J. W. Suppression of the Ag/Si Surface Conductivity Transition Temperature by Organic Adsorbates. *Appl. Phys. Lett.* **2011**, *98*, 052106.
73. Perdew, J. P.; Zunger, A. Self-Interaction Correction to Density-Functional Approximations for Many-Electron Systems. *Phys. Rev. B* **1981**, *23*, 5048–5079.
74. Koerzdoerfer, T. On the Relation between Orbital-Localization and Self-Interaction Errors in the Density Functional Theory Treatment of Organic Semiconductors. *J. Chem. Phys.* **2011**, *134*, 094111.
75. Hofmann, D.; Koerzdoerfer, T.; Kuemmel, S. Kohn−Sham Self-Interaction Correction in Real Time. *Phys. Rev. Lett.* **2012**, *108*, 146401.
76. Marom, N.; Kronik, L. Density Functional Theory of Transition Metal Phthalocyanines, I: Electronic Structure of NiPc and CoPc-Self-Interaction Effect. *Appl. Phys. A* **2009**, *95*, 159–163.
77. Graetzel, M.; Frank, A. J. Interfacial Electron-Transfer Reactions in Colloidal Semiconductor Dispersions. Kinetic Analysis. *J. Phys. Chem.* **1982**, *86*, 2964–2967.
78. Feenstra, R. M.; Stroscio, J. A. Tunneling Spectroscopy of the GaAs(110) Surface. *J. Vac. Sci. Technol. B* **1987**, *5*, 923–929.
79. Berthe, M.; Stiufiuc, R.; Grandidier, B.; Deresmes, D.; Delerue, C.; Stiévenard, D. Probing the Carrier Capture Rate of a Single Quantum Level. *Science* **2008**, *319*, 436–438.
80. Toader, M.; Knupfer, M.; Zahn, D. R. T.; Hietschold, M. Initial Growth of Lutetium(III) Bis-Phthalocyanine on Ag(111) Surface. *J. Am. Chem. Soc.* **2011**, *133*, 5538–5544.
81. Wang, B.; Wang, K. D.; Lu, W.; Wang, H. Q.; Li, Z. Y.; Yang, J. L.; Hou, J. G. Effects of Discrete Energy Levels on Single-Electron Tunneling in Coupled Metal Particles. *Appl. Phys. Lett.* **2003**, *82*, 3767–3769.
82. Xue, Y.; Datta, S.; Hong, S.; Reifenberger, R.; Henderson, J. I.; Kubiak, C. P. Negative Differential Resistance in the Scanning-Tunneling Spectroscopy of Organic Molecules. *Phys. Rev. B* **1999**, *59*, R7852–R7855.
83. Fang, Y.-K.; Liu, C.-L.; Li, C. X.; Lin, C.; Mezzenga, R.; Chen, W.-C. Synthesis, Morphology, and Properties of Poly(3-Hexylthiophene)-*Block*-Poly(Vinylphenyl Oxadiazole) Donor−Acceptor Rod−Coil Block Copolymers and Their Memory Device Applications. *Adv. Funct. Mater.* **2010**, *20*, 3012–3024.
84. Nacci, C.; Fölsch, S.; Zenichowski, K.; Dokić, J.; Klamroth, T.; Saalfrank, P. Current *versus* Temperature-Induced Switching in a Single-Molecule Tunnel Junction: 1,5 Cyclooctadiene on Si(001). *Nano Lett.* **2009**, *9*, 2996–3000.
85. Pitters, J. L.; Wolkow, R. A. Detailed Studies of Molecular Conductance Using Atomic Resolution Scanning Tunneling Microscopy. *Nano Lett.* **2006**, *6*, 390–397.
86. Gaudioso, J; Lauhon, L. J.; Ho, W. Vibrationally Mediated Negative Differential Resistance in a Single Molecule. *Phys. Rev. Lett.* **2000**, *85*, 1918–1921.
87. Donhauser, Z. J.; Mantooth, B. A.; Kelly, K. F.; Bumm, L. A.; Monnell, J. D.; Stapleton, J. J.; Price, D. W., Jr.; Rawlett, A. M.;

Allara, D. L.; Tour, J. M.; *et al.* Conductance Switching in Single Molecules Through Conformational Changes. *Science* **2001**, *292*, 2303–2307.
88. Gaudioso, J.; Ho, W. Steric Turnoff of Vibrationally Mediated Negative Differential Resistance in a Single Molecule. *Angew. Chem., Int. Ed.* **2001**, *40*, 4080–4082.
89. Chen, J.; Reed, M. A.; Rawlett, A. M.; Tour, J. M. Large On-Off Ratios and Negative Differential Resistance in a Molecular Electronic Device. *Science* **1999**, *286*, 1550–1552.
90. Chen, L.; Hu, Z.; Zhao, A.; Wang, B.; Luo, Y.; Yang, J.; Hou, J. G. Mechanism for Negative Differential Resistance in Molecular Electronic Devices: Local Orbital Symmetry Matching. *Phys. Rev. Lett.* **2007**, *99*, 146803.
91. Tu, X. W.; Mikaelian, G.; Ho, W. Controlling Single-Molecule Negative Differential Resistance in a Double-Barrier Tunnel Junction. *Phys. Rev. Lett.* **2008**, *100*, 126807.
92. Yao, J.; Zhong, L.; Natelson, D.; Tour, J. M. Silicon Oxide: A Non-innocent Surface for Molecular Electronics and Nanoelectronics Studies. *J. Am. Chem. Soc.* **2011**, *133*, 941–948.
93. Yao, J.; Sun, Z.; Zhong, L.; Natelson, D.; Tour, J. M. Resistive Switches and Memories from Silicon Oxide. *Nano Lett.* **2010**, *10*, 4105–4110.
94. Kresse, G.; Hafner, J. *Ab Initio* Molecular Dynamics for Liquid Metals. *Phys. Rev. B* **1993**, *47*, 558–561.
95. Vanderbilt, D. Soft Self-Consistent Pseudopotentials in a Generalized Eigenvalue Formalism. *Phys. Rev. B* **1990**, *41*, 7892–7895.
96. Monkhorst, H. J.; Pack, J. D. Special Points for Brillouin-Zone Integrations. *Phys. Rev. B* **1976**, *13*, 5188–5192.